5-2015

The characterization of amyloid fibrils and novel synthetic heparin-binding peptides binding to cell surfaces

Nicole Marie Hackenbrack
nhackenb@vols.utk.edu

Follow this and additional works at: https://trace.tennessee.edu/utk_chanhonoproj

Part of the Amino Acids, Peptides, and Proteins Commons, Biochemistry Commons, Cardiovascular Diseases Commons, Cell Biology Commons, Cellular and Molecular Physiology Commons, Diagnosis Commons, and the Therapeutics Commons

The characterization of amyloid fibrils and novel synthetic heparin-binding peptides binding to cell surfaces

Nicole Hackenbrack
Department of Medicine, University of Tennessee Graduate School of Medicine, Knoxville, TN
Thesis, University of Tennessee Knoxville, Chancellor's Honors Program

Introduction

Proteins are dynamic structures which fold based on local and global characteristics to find the lowest energy state. Through non-covalent interactions, hydrophobic regions generally crowd towards the middle to promote the formation of functional, soluble "native" proteins (Ramirez-Alvarado, 4). Once the protein has performed its function, proteases degrade the protein, so that the amino acids can be recycled and the intracellular protein concentration remains controlled. When this balance is tampered with, disease may develop.

Proteins misfold in response to unfavorable environmental conditions or with the presence of specific genomic mutations. The misfolded proteins may aggregate, as the mistakenly formed hydrophobic β-pleated sheet secondary structures stack to form amyloid fibrils (Merlini, 2003). Thermodynamically, the monomeric proteins in amyloid fibrils are at the lowest energy state (Ramirez-Alvarado, 5). These fibrils are resistant to protease activity and cause a number of physiological problems, including cytotoxicity and oxidative stress (Merlini, 2003). Amyloidosis is associated with over 20 proteins and is responsible for a broad range of pathologies, including neurodegenerative diseases, rheumatoid arthritis, cystic fibrosis, multiple myeloma and Type II Diabetes. Unfortunately, there are no FDA-approved imaging or therapeutic agents for systemic amyloid and the only true method of diagnosis is a biopsy or autopsy (Wall, 2011).

As amyloid fibril matures, apolipoprotein E, glycosaminoglycans (GAG) and serum amyloid P component (SAP) associate with the amyloid deposit. In fact, in Europe, radiolabeled SAP is used as a diagnostic imaging tool for amyloidosis (Ancsin, 2003). Heparan sulfate is a type of GAG that makes up heparan sulfate proteoglycans (HSPG), a ubiquitous extracellular matrix component that binds to a range of ligands, such as growth factors and a variety of viruses (Ancsin, 2003; Gandhi, 2008). It has been shown that HSPG associated with amyloid are highly sulfated and exhibit a change in the proportion of disaccharides when compared to HSPG in healthy individuals (Wall, 2012; Lindahl, 1997). For this reason, HSPG have the potential to serve as useful biomarkers for amyloid imaging and therapy.

In vitro and *in situ* imaging of amyloid is usually performed with Thioflavin T and Congo red, respectively (Kisilevsky, 2007). However, it has been difficult to develop *in vivo* imaging and therapeutic techniques due to a lack of knowledge about the mechanisms of amyloidosis. In order to better study, diagnose and treat amyloidosis, a series of novel synthetic peptides directed at the amyloid-bound GAG were engineered.

Synthetic Peptides

The synthetic heparin-binding peptides used in this study are derivatives of protamine (P1). Protamine sulfate is an FDA-approved antagonist of heparin and is used inactivate the anticoagulant effects of heparin (Chargaff, 1938). Novel synthetic peptides were designed so that their positively charged residues, arginine or lysine, are 3 or 4 residues apart (Table 1). The neutral alanine and glutamine residues are in between, which allows the peptide to fold into an α-helical structure. This means that the positive residues are concentrated on one face of the helix (Figure 1). Theoretically, this concentrated positive charge has a strong preferential affinity to the negatively charged, hypersulfated HSPG associated with amyloid in the extracellular matrix. In contrast, negative control peptides were prepared to mimic the amino acid sequence of the heparin-binding peptides, but instead replace the positively charged lysine and arginine residues with alanine or glycine.

Novel Synthetic Heparin-Binding Peptide Sequences	
Peptide	Sequence
P1	CGGYS SSRPV RRRRR PRVSR RRRRG GRRRR
P5+14	CGGYS KAQKA QAKQA KQAQK AQKAQ AKQAK QAQKA QKAQA KQAKQ
P5R+14	GGGYS RAQRA QARQA RQAQR AQRAQ ARQAR QAQRA QRAQA RQARA
P31G	CGGYS GAQGA QAGQA GQAQG AQGAQ AGQAG Q

Table 1. The amino acid sequences of protamine (P1), synthetic peptides that bind to heparin (P5+14 and P5R+14), and the negative control peptide (P31G).
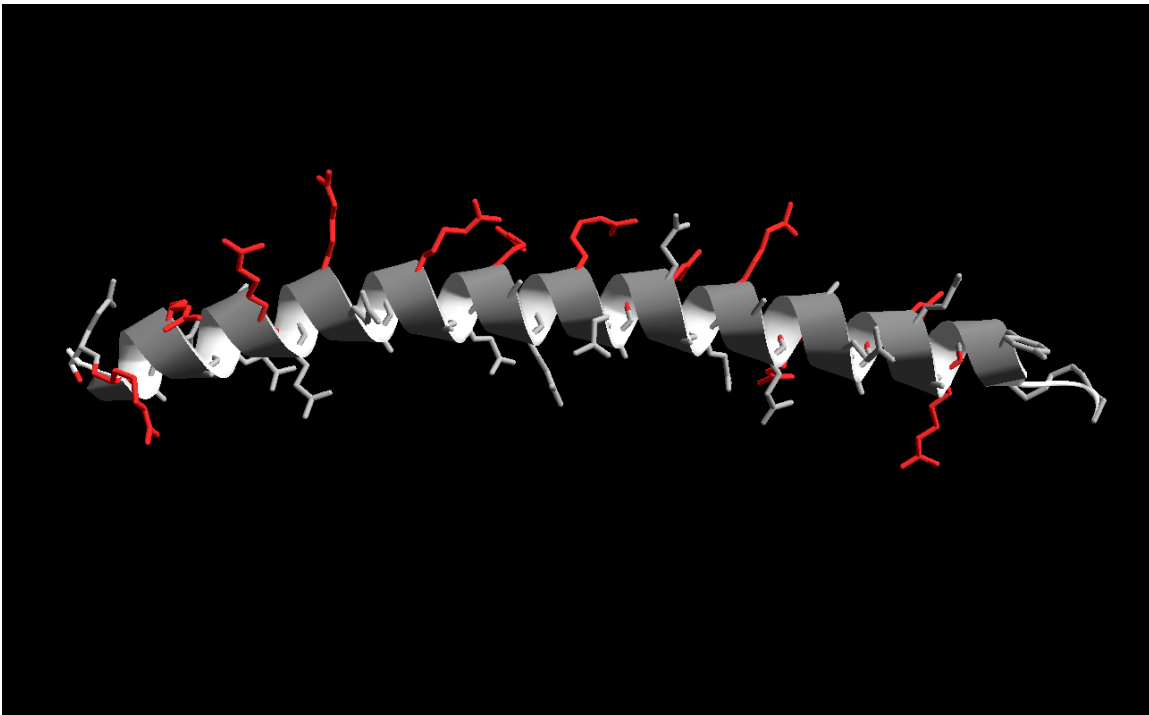

Figure 1. A computer model of the structure of P5R+14, showing the localization of positive arginine residues (red) on one side of the α-helical structure.

These peptides can be biotinylated, or covalently bonded to biotin, via their CGGYS leader sequence. Biotin binds tightly and rapidly to streptavidin, which can be labeled with the

fluorogenic europium (Dahlen, 1987). For this reason, these heparin-binding peptides serve as sensitive and reliable reagents for *in vitro* assays.

Heparan Sulfate Proteoglycans (HSPG)
Previous research has implicated HSPG's role in amyloid fibril deposition (Fraser, 1992), stabilization (Yamaguchi, 2003), fibrillization (Ancsin, 1999; Castillo, 1998) and protection from proteolysis (Gupta-Bansal, 1995). In order to perform these functions, it has been suggested that HSPG binds to the secondary structure of monomeric amyloidogenic proteins in addition to associating with amyloid fibrils (Ancsin, 2003).

Upon closer examination of the amyloid-associated HSPG, it was concluded that more HSPG is present in amyloid-associated organs, and that HSPG in amyloid-associated organs differ in composition from healthy organs. It has been suggested that subclasses of HSPG, such as perlecan or syndecan, may dictate the organ specificity of amyloid deposition (Lindahl, 1997). Unfortunately, the high variability of sulfation and other modifications on heparan sulfate chains has made it difficult to perform structural analyses and reveal the specific interactions with amyloidogenic proteins and amyloid fibrils (Ramirez-Alvarado, 562). HSPG biosynthesis is another topic that remains elusive. Altered HSPG biosynthesis associated with amyloid deposition might reflect altered transcription or modification steps, but longitudinal studies that study HSPG before and during amyloidogenesis are necessary to explain the relationship between HSPG biosynthesis and amyloid (Ancsin, 2003).

This portion of our study focuses on gaining a clearer understanding of how synthetic heparin-binding peptides and/or amyloid fibrils bind to the cell surface. In addition, we will explore peptide binding directly to the fibrils. We hypothesize that the peptides bind to HSPG and amyloid fibrils by interacting with their negatively charged regions. Furthermore, we suspect that they have the highest affinity for the hypersulfated, and therefore extremely negatively charged, amyloid-associated HSPG.

AL Amyloidosis
In addition to our studies of peptide binding, we also wish to investigate amyloid fibril interactions at cell surfaces as related to systemic light chain amyloidosis. Light chain amyloidosis, also known as AL or primary amyloidosis, is the fibrillization and circulation of monoclonal amyloidogenic immunoglobulin light chains, usually consisting of the N-terminal variable domain of the light chain protein (Ramirez-Alvarado, 333). Mutations in various regions that contribute to AL protein instability have been identified, and overproduction and proteolytic cleavage of the AL protein have also been recognized as possible mechanisms contributing to amyloidogenesis (Ramirez-Alvarado, 329-334). This systemic amyloidosis generally manifests as protein deposits in heart, liver, and kidney tissue, although the tissue specificity of deposition is not well understood (Sanchorawala, 2006).

Approximately 50% of AL patients develop cardiac amyloidosis, which can form in the atria, ventricles, and coronary vessels (McWilliams-Koeppen). Early symptoms have been described as "flu-like," and progress into abnormal electrocardiography (ECG) due to increased wall thickness, chest pain, abnormal bleeding, and dizziness from hypotension, along with other symptoms arising from multiorgan involvement (Dubrey, 1998; Mumford, 2000). Current

treatments target the plasma cells that produce the monoclonal light chain proteins through chemotherapy and stem cell transplant, but the fact remains that sudden heart failure is the most common cause of death in these patients (Lacy, 2008; Dubrey, 1998).

In Vitro Studies of AL Amyloidosis

Cardiac amyloidosis is under-diagnosed and more effective treatments are called for. With an aim to better understand the mechanisms of cardiac damage in light chain amyloidosis, and to explore any utility of our heparin-binding peptides with respect to this disease, we have undertaken studies in a cell culture system with immortalized cardiomyocytes (AC10) and an amyloidogenic protein cloned from an AL patient with cardiac involvement.

Taken together the studies outlined here provide a preliminary evaluation of cell surface interactions relating both to fibril deposition in AL and the binding of synthetic peptides targeted to cell surface HSPG associated with systemic amyloidosis. These findings serve as a foundation for future research dedicated to understanding amyloid deposition and pathogenesis and the development of imaging and therapeutic reagents.

<u>Methods and Materials</u>
Plating Cells
Adult human ventricular cardiomyocytes (AC10), mouse embryonic fibroblast cells (MEF), Chinese hamster ovary cells (CHO), human liver carcinoma cells (HepG2) or human breast cancer cells (MCF7) were cultured in complete DMEM/F12 medium (Lonza) supplemented with 5% fetal bovine serum and penicillin (100 units/mL)-streptomycin (100 µg/mL)-gentamicin (10 µg/mL) and plated at 30% confluency on glass coverslips and cultured for 48 hours at 37°C.

Fixed Cell Assay of Peptide Binding
MEF in a 96 well tissue culture plate were washed once with 200 µL per well of phosphate buffered saline (PBS). The cells were fixed using 75 µL per well of 1.25% glutaraldehyde for 20 minutes at room temperature. The plate was washed as before twice with 200 µL of PBS in each well. In some cases Tris buffered saline (TBS) was used instead to ensure inactivation of the fixative. Cells were stored at 4°C in PBS or assayed immediately.

The cells were blocked with 200 µL of 1% bovine serum albumin (BSA)/PBS or BSA/TBS. The plate was incubated with 100 µL per well of peptides p5R+14 and p31G either in dilutions or at a single concentration of 0.5 µg/mL of 0.1% BSA/PBS for 60-90 minutes at room temperature. The plate was washed three times with PBS as before. The cells were probed with 100 µL of Europium-conjugated streptavidin in PBS/0.1% BSA for 30 minutes at room temperature. The plate was washed three times with PBS, Europium enhancement solution added, and time resolved fluorescence measured on the Wallac Victor 3. Europium is a lanthanide chelate label, which has a long decay time, optimal for reducing autofluorescent background noise with the use of time resolved fluorescence (Perkin-Elmer).

Enzyme Treatment
Heparinases I, II, and III and chondroitinase ABC, ordered from Sigma-Aldrich, were hydrated in Tris-buffered saline (TBS) as recommended by the manufacturer. They were stored at -80°C in aliquots. Before fixation cultured cells were washed twice in DMEM/F12 containing no serum or antibiotics. Enzymes (100 µL/well) were added at 0.5 units/mL in DMEM/F12 and incubated for 90 minutes at 37°C. Cultures were then either fixed, as noted in the preceding section, or probed directly with biotinylated peptides p5R+14 and p31G, as described below.

Live Cell Assay of Peptide Binding
For probing of unfixed MEF, cells were washed twice in ice cold DMEM/F12 containing no serum or antibodies. Each well was probed with 100 µL of 0.5 µg/mL in cold DMEM/F12 with 0.1% BSA and incubated for one hour at 4°C. Wells were then washed with ice cold PBS (200 µL per well) and fixed with 1.25% glutaraldehyde as noted above, washed twice, and stored in PBS for 24 hours. Cultures were washed once with PBS and blocked with 1% BSA in PBS at 100 µL per well. Finally, the cultures were probed with streptavidin europium as stated above.

Heparin Inhibition of Peptide Binding
All wells were filled with 100 µL of cold DMEM/F12 medium. The appropriate wells were filled with more solution and then either 3 µL of Lovenox or 25 µL of heparin for a total of 150 µL per well. 50µL was transferred to the next row of wells and down the plate as a 3-fold dilution series. Immediately following, 50 µL solutions of P5+14 and P5G (20 µL in 6 mL DMEM/F12 and 3µL

in 1 mL, respectively) were added to each well. The cells incubated with heparin or Lovenox and peptides for one hour at 4°C. The plate was then washed three times with 100 µL of PBS. The cells were fixed with 50 µL of glutaraldehyde for 20 minutes. The plate was washed again and blocked for one hour with 150 µL of 1% BSA/PBS+glycine. The plate was washed again and 100 µL streptavidin in 0.1% BSA/PBS (at 5 µL/10 mL) was added. After 30 minutes, the plate was washed again and 100 µL of enhancement solution was added.

Heparin Inhibition of Wil Fibrils
Wil fibrils, sonicated at about 50%, were plated to 1 µg per well on a 96 well ELISA plate and incubated overnight at 4°C. They were blocked with 1% BSA/PBS with 200 µL per well. After an hour, the plate was washed. All wells were filled with 100 µL of 1% BSA/PBS in wash/detergent ("wash"). The appropriate wells were filled with more solution and then either 3 µL of Lovenox or 25 µL of heparin for a total of 150 µL per well. 50µL was transferred to the next row of wells and down the plate as a 3-fold dilution series. Immediately following, 50 µL solutions of P5+14 and P5G (20µL in 6 mL of wash and 3µL in 1 mL, respectively) were added to each well. The cells incubated with heparin or Lovenox and peptides for one hour. The plate was then washed three times with the wash. 100 µL of streptavidin (at 5 µL/10mL of wash) was added to each well and incubated covered for 30 minutes. 100 µL of enhancement solution was added.

Fluorescent Fibril Binding on AC10 Cells
In each experiment, the cells were fixed in 4% paraformaldehyde (pre-prepared by Becton-Dickenson) for 20 minutes after being washed in PBS. The cells were then permeabilized with 0.2% Triton X-100 in PBS for 5 minutes. After being washed twice with PBS, the cells were blocked with 1% BSA in PBS for at least 30 minutes.

In the binding assays, the cells were incubated with AlexaFluor 594-phalloidin in 1% BSA/PBS for 1 hour to allow visualization of the cellular cytoskeleton. In assays assessing the mitochondrial function in Wil fibril-treated cells, the cells were incubated with 0.3 µL of MitoTracker Red for 30 minutes. Finally, the cells were washed once and treated with Hoechst 33342 in PBS for 5 minutes for staining of cell nuclei.

Microscopy Procedure
After the cells were washed twice, they were placed on slides with fluorescent mounting medium (DAKO). The cells were either observed under a Leitz DMRB microscope from and photos were acquired using a SPOT RT3 camera from Diagnostic Instruments Inc., or the slides were sent to Oak Ridge National Laboratory to be imaged using a LSM 710 confocal laser scanning microscope. The Z-step distance was 0.1 µm.

MTT Assay of Mitochondrial Function
AC10 cells were plated on a 96 well tissue culture plate. After incubation with Wil fibrils, the cells were incubated in 50 µL of MTT for 3 hours. The medium was then removed and the insoluble MTT oxidative product solubilized in 0.5 mL of isopropanol. The absorbance at 540 nm was measured on an ELISA reader.

Preparation of Synthetic AL Amyloid Fibrils
RNA was isolated from a plasma cell of an AL amyloidosis patient with cardiac involvement, which was then amplified using variable domain λ6 light chain-specific primers and cloned into *E. coli* expression plasmid. The AL protein (recombinant variable domain λ6 light chain, $rV_\lambda6Wil$) was expressed and purified, as previously described (Wall, 1999). Finally, amyloid fibrils were prepared, using a mixture of unlabeled monomers with Alexa-Fluor 488 (Life Technologies) fluorescently labeled monomers (McWilliams-Koeppen). These fibrils will hereafter be referred to as Wil fibril.

<u>Results</u>
Synthetic Peptide Binding
In order to test the role of positive-charged amino acids on the heparin-binding peptide backbone, binding of peptides p5R+14 and p31G, the negative control peptide, was compared on fixed MEF cells. We predicted that p5R+14 would bind in a dose-dependent manner based on the presumption that charge binding was the primary interaction between its positively charged arginine residues and the negatively charged extracellular matrix. At a peptide concentration of 0.0625 μg/mL, p5R+14 binding began to increase dramatically and deviate from the p31G binding pattern (Figure 2). The neutral control peptide p31G did not experience the same clear increase in binding at higher concentrations. At a peptide concentration of 1 μg/mL, fluorescence output from p5R+14 binding was four times that of p31G.
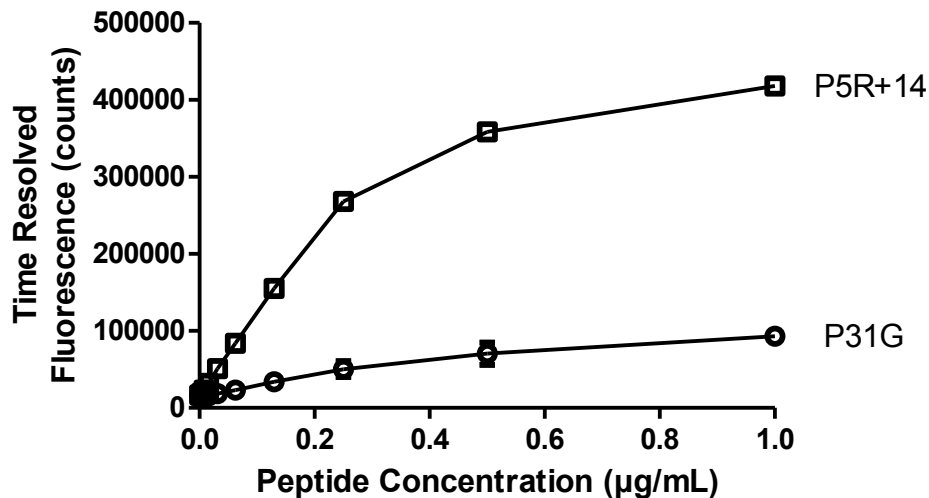

Figure 2. P5R+14 Binding in a Dose-Dependent Manner. MEF cells were fixed with 1.25% glutaraldehyde and washed with PBS. Cells were blocked with 200 μL of 0.1% BSA/PBS. 200 μL of peptides were added to the first column at 2 μg/mL in 0.2% BSA/PBS and 100 μL was transferred down the plate in 2-fold dilutions, excluding the last column.

Because fixation is a harsh treatment that potentially results in physiologically inaccurate depiction of cell surface binding, peptide p5R+14 and p31G binding was compared again with a live cell assay. This assay was carried out in cold temperatures to decrease plasma membrane fluidity and prevent peptide internalization, in order to get an accurate measurement of peptide binding on the cell surface. Again, a steady increase in p5R+14 binding is observed, while p31G binding remains constant (Figure 3). In addition, these fluorescence counts correspond to those in the fixation assay dataset.
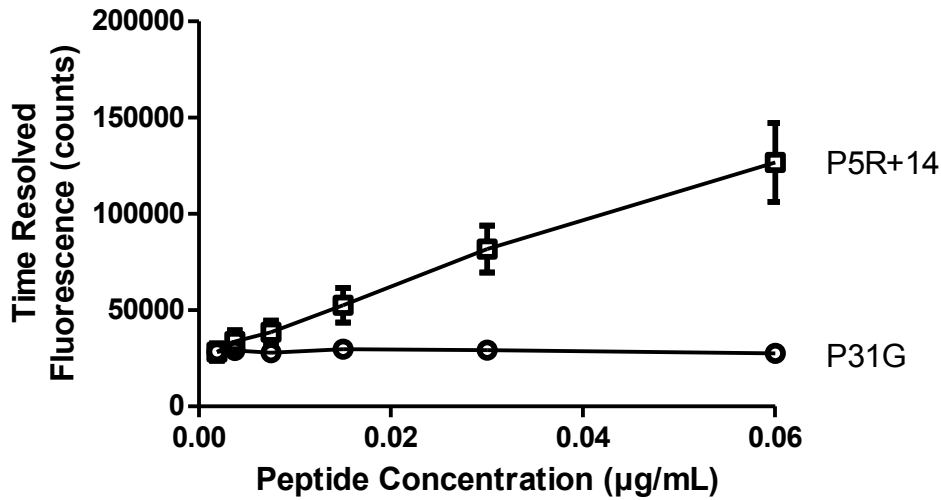
Figure 3. P5R+14 Binding Analysis with a Live Cell Assay. Peptides, medium, and plate kept on ice until fixation. MEF cells were washed in cold 0.2% BSA/DMEM-F12 once. 100 μL of cold DMEM-F12 medium was added to each well. 200 μL of peptides were added at 2 μg/mL to first column. 100 μL was transferred down the plate in a dilution series. After an hour on ice, wash with PBS and fix with 1.25% glutaraldehyde. After fixation, the plate was washed twice with 100 μL of TBS and bound peptide assayed.

In order to visualize peptide binding, light microscopy was utilized to compare the binding of p5+14, which contains lysine residues, and p31G (Figure 4). At a concentration of 0.5 μg/mL, green fluorescent p5+14 bound, but not uniformly, to the HepG2 cells. However, there was no visible fluorescence present on the cells that were treated with fluorescently labeled p31G. Time-dependent binding of p5+14 to CHO cells was also observed (Figure 5). Between 6 and 24 hours of incubation with green fluorescently labeled p5+14, there is a significant increase in the amount of p5+14 bound to the cells. Green fluorescent p5+14 can still be observed to a lesser extent at the 30 minute, 1 hour, and 3 hour time points. However, no p31G bound to the cells after a 24-hour incubation period.
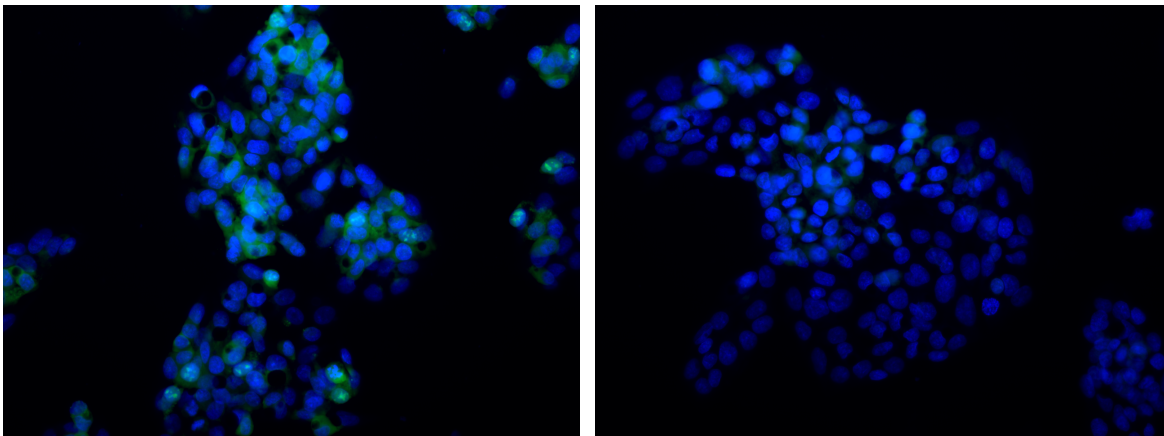

Figure 4. Visualization of P5+14 Binding. HepG2 cells incubated with 0.5 μg/mL of fluorescently labeled peptide (green) (A) P5+14 or (B) P31G, shown at 400X magnification. The peptides appear green, while the nuclei are stained blue from their treatment with Hoechst 33342.
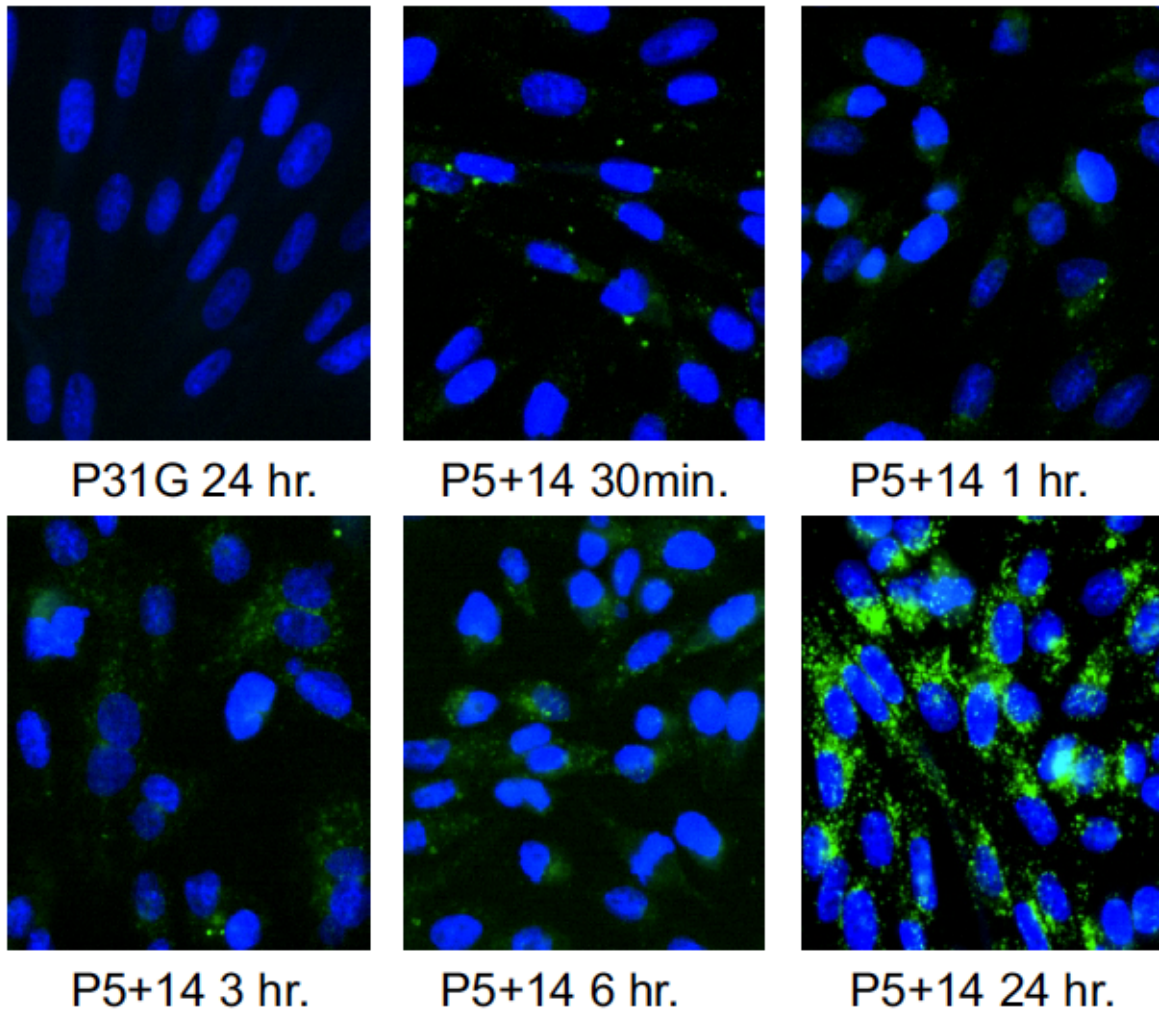
Figure 5. Visualization of Time-Dependent Binding of P5+14. CHO cells were incubated with 0.5 μg/mL of fluorescently labeled P5+14 (green) for 30 minutes, 1, 3, 6, and 24 hours on poly-L lysine (PLL) coated plates.

The Role of HSPG in Peptide Binding
In order to investigate the role of HSPG on peptide binding, HSPG were digested using three heparinase isozymes, which cleave the heparan sulfate at specific points in the saccharide sequence (Figure 6). Due to the fact that amyloid-associated HSPG have a distinct disaccharide sequence, treatment with the three isozymes, heparinase I, II, and III, may result in different binding affinities. For the sake of comparison, chondroitin sulfate was also digested with chondroitinase. Chondroitin sulfate is a galactosaminoglycan that also forms proteoglycans in the extracellular matrix.
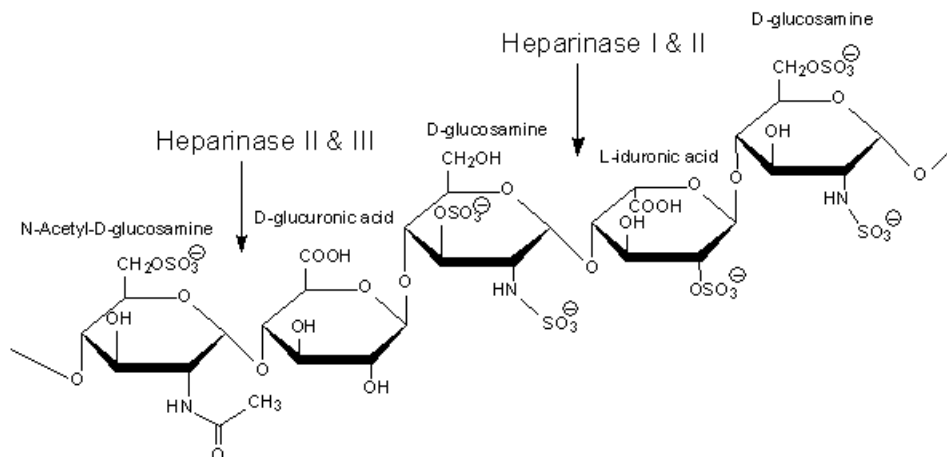
Figure 6. A generic saccharide sequence of heparan sulfate and the bonds cleaved by the types of heparinases (Source: http://www.sigmaaldrich.com/life-science/metabolomics/enzyme-explorer/learning-center/carbohydrate-analysis/carbohydrate-analysis-iii.html)

Based on the number of cleavage sites, a decrease in binding affinity would be expected when using either heparinase I or III, while a greater reduction in peptide binding would be expected when using heparinase II. However, in tests using heparinase I, II, and III individually or heparinase I and II in combination, peptide binding decreased by about 40%. In addition, chondroitinase caused about a 10% reduction in peptide binding (Figure 7).
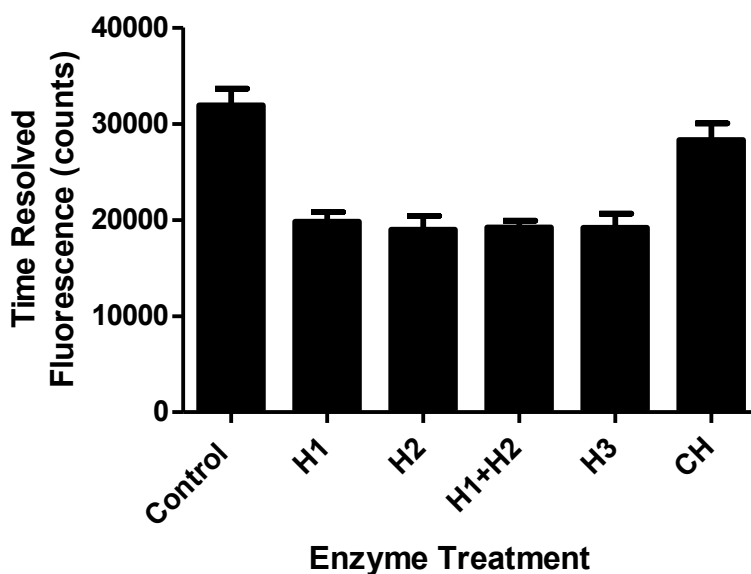

Figure 7. Enzyme Treatment of Cell Surface HSPG. 0.8 mL of DMEM-F12 medium was added to test tubes. 0.5 units/mL of heparanase I (H1), heparanase II (H2), heparanase III (H3), or chondroitinase ABC (CH) and 0.5 units/mL H1 or 0.5 units/mL H2 (H1+H2) were added to separate test tubes. 80 μL of of each was added to a column of wells already containing 20 μL of medium. The plate was incubated (37°C) for an hour and a half. MEF cells were washed once with cold 0.1% BSA/DMEM-F12 medium. Biotinylated peptides were added at 1 μg/mL and binding assayed. The values shown are based on the fluorescence of p31G subtracted from that of p5R+14 as a background count. T-tests revealed that cells treated with H1, H2, H1+H2, and H3 are significantly different from untreated cells at $p<0.001$ and cells treated with CH is significantly different from untreated cells at $p<0.01$.

It is possible that the heparin isozymes were not efficient at digesting the cell surface HSPG. In order to better depict the role HSPG plays in peptide binding, peptide binding to cells that present variable amounts of GAG on the cell surface was analyzed. GAG biosynthesis is well studied in CHO cells, and variant CHO cell lines with deficient GAG synthesis are available and represent an ideal choice to study peptide binding with respect to HSPG. A deficiency in transferases needed for GAG biosynthesis alters the concentration of HSPG on the cell surface (Silva, 2013; Table 2). Assuming that peptide P5+14 only binds to HSPG, the fluorescence output of P5+14 bound to the B761 variant of CHO cells should be less than when bound to the control CHO cells. In addition, we would not expect any P5+14 to bind to the cells devoid of HSPG (A745 and D677 variants). When cells were incubated with 0.5 µg/mL of P5+14, B761 cells experienced only about 80% of control binding levels, while peptide binding was reduced by 40% on both A745 and D677 cells (Figure 8). When performed over a concentration gradient, the test yielded similar results (Figure 9).

CHO Variant Cell Lines		
Cell Line	Deficiency	Expression of GAGs
K1	None - Parent Line	Control, or Wild Type
A745	xylosyltransferase	Lacks expression of all GAGs
B761	galactosyltranferase I	5% of Wild Type chondroitin and heparan sulfate
D677	N-acetylglucosaminyltransferase and glucuronosyltransferase	300% of chondroitin sulfate and lacks expression of heparan sulfate

Table 2. A summary of the biosynthesis of GAGs in various CHO variant cell lines. Information adapted from Silva, et al. (2013).
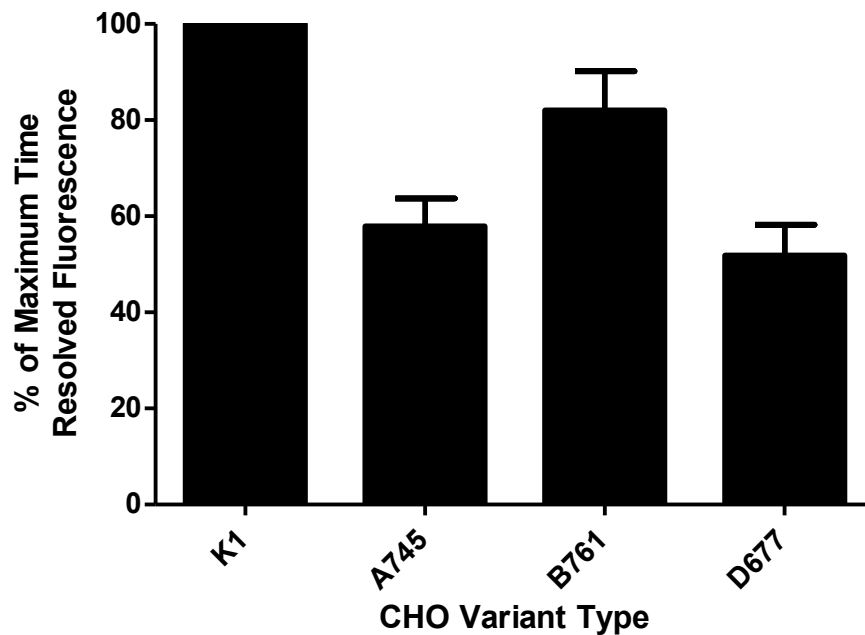

Figure 8. Peptide Binding on CHO Variants. CHO variants, which have different heparan and chondroitin sulfate concentrations, were assayed for binding of 0.5 µg/mL P5+14.
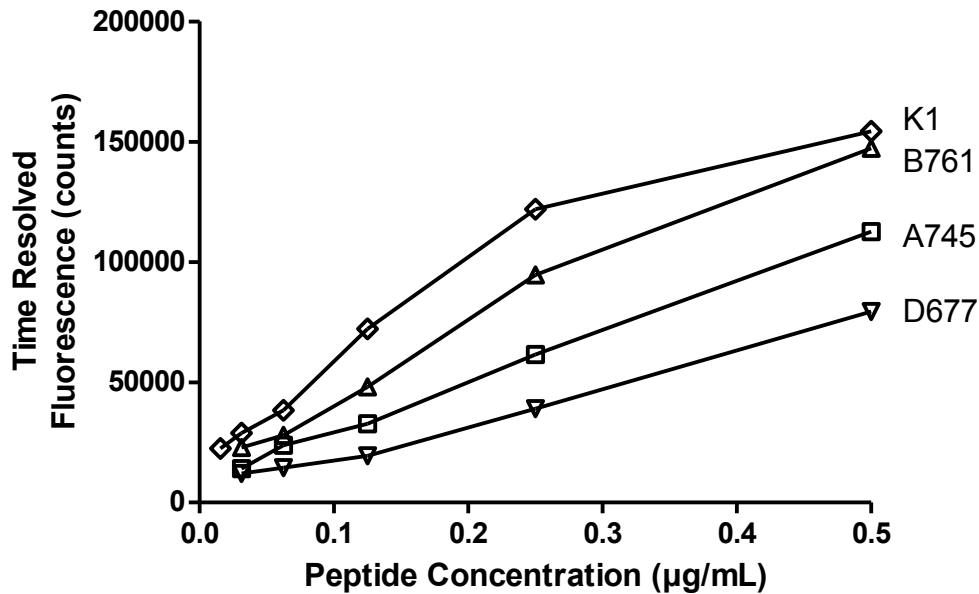
Figure 9. Dose-Dependent Peptide Binding to CHO Variants. CHO variants, which have different haparan and chondroitin sulfate concentrations, were incubated with varying concentrations of P5+14 and peptide binding measured.

Peptide Binding Inhibition with Heparin

In addition to binding with the HSPG in the extracellular matrix, the heparin-binding synthetic peptides have been shown to bind directly to amyloid fibrils in the absence of associated HSPG (Wall, 2015). The positive charges of the peptide align with the residues extending from the fibril core structure of β-pleated sheets (Figure 10). We sought to compare the peptide binding on the Wil fibrils to binding to CHO cells and to a natural preparation of fibrils from human tissue, or Cab Amyloid. Peptide P5+14 binding inhibition with heparin was used as the measure to compare the relative strength of the bond between the peptide and the cell surface, Cab Amyloid or Wil fibril (Figure 11). More heparin was required to inhibit peptide binding to Wil fibrils than was required to inhibit binding to CHO cells and Cab Amyloid. Inhibition of peptide binding to CHO cells required the lowest concentration of heparin. This heparin-binding peptide binds with the highest affinity to Wil fibrils, moderately binds to Cab Amyloid, and has the lowest affinity for the CHO cell surface.
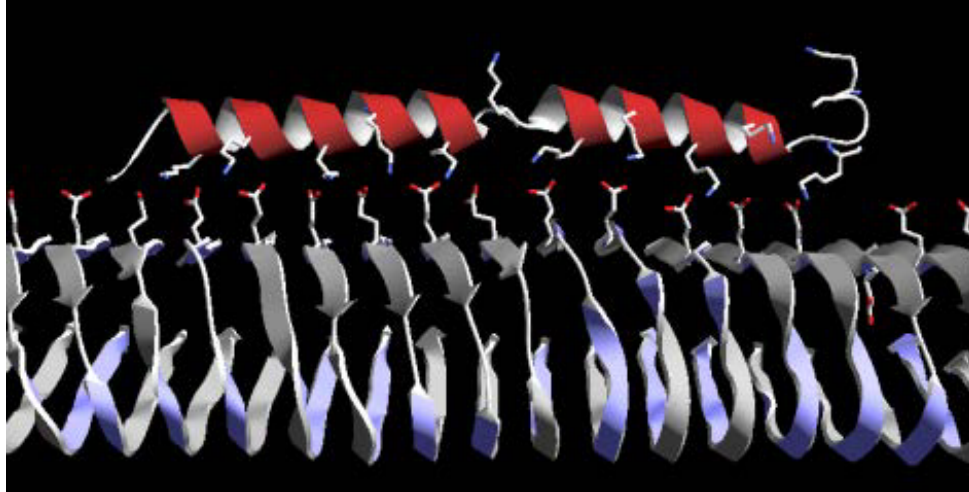
Figure 10. Computer generated model for peptide and binding on Aβ fibril binding. Peptide p5+14 binds directly to the fibrils, due to interactions between lysine sidechains on peptide and glutamate side chains on Aβ monomers (Wall, 2015). This image was generated was performed by collaborators at the Oak Ridge National Laboratory.
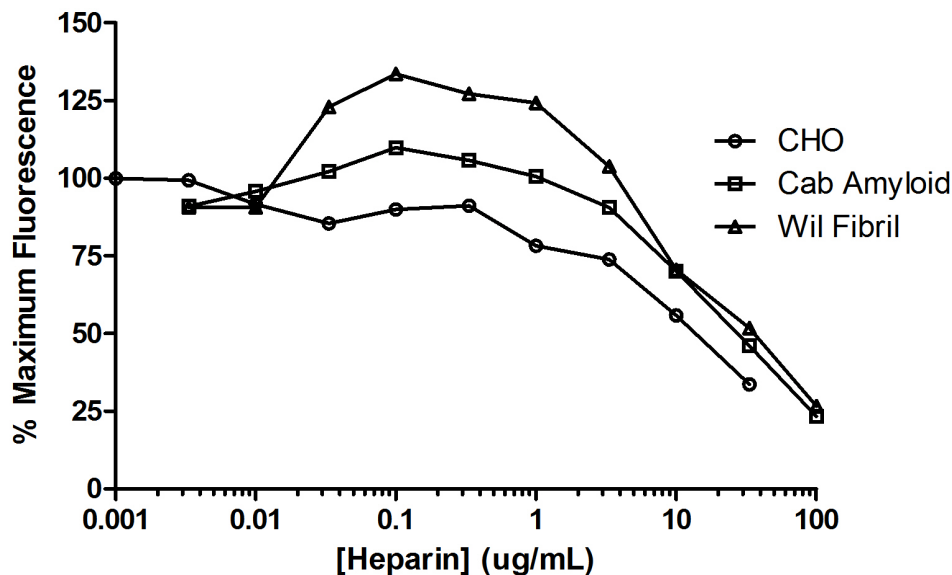

Figure 11. Peptide P5+14 Binding Inhibition by Heparin. CHO cells, Cab Amyloid, or Wil fibrils were incubated with 0.5 μg/mL of peptide P5+14 and various concentrations of heparin for one hour. The percent of the maximum time resolved fluorescence output for each substrate is shown.

Now, we turned our attention to the binding of peptides on cardiomyocytes (AC10), in order to begin an exploration of cell surface binding in AL amyloidosis. Amyloid-associated HSPG has been described as heparin-like because of its hypersulfation. Heparin and low molecular weight heparin, Lovenox, were incubated alongside the synthetic peptide, in order to test whether binding of the peptide P5+14 to the HSPG on the cell surface is inhibited by heparins in solution (Figure 12). Concentration-dependent inhibition of peptide binding was observed, and Lovenox proved to be the stronger inhibitor. In order to confirm that the peptide and heparin were binding to each other in solution and that the heparins were not binding to and potentially altering the cell surface, a "wash out" procedure was developed, in which the cells were incubated with the heparins for one hour, washed, and then incubated with the peptide. Peptide binding remained

constant over several concentrations of heparins, verifying that the peptide and heparins bind in solution (Data not shown).
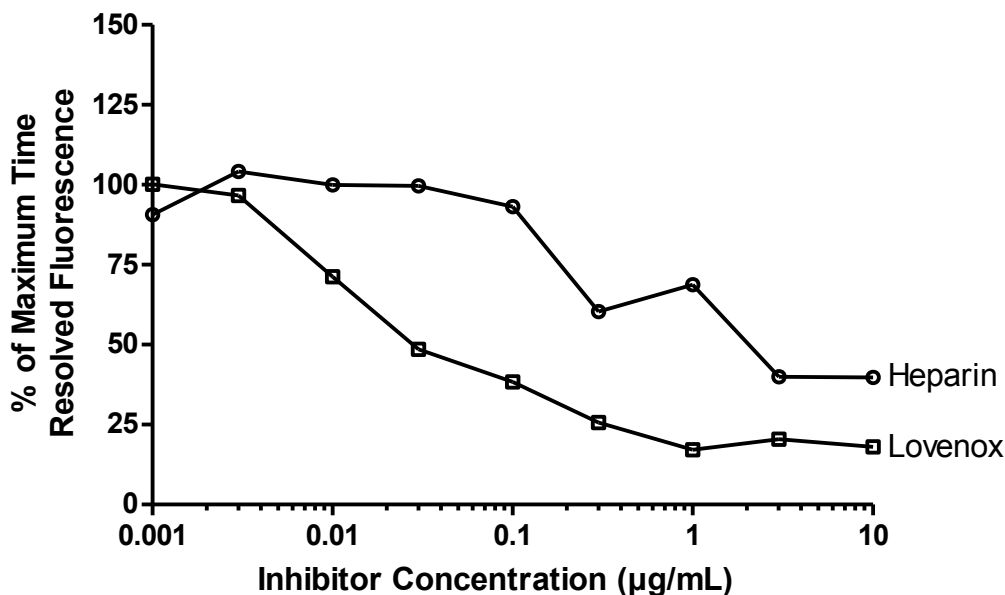

Figure 12. Inhibition of Peptide Binding with Heparins. AC10 cells were incubated with peptide P5+14 and various concentrations of heparins for one hour.

Peptide P5+14 binds the strongest to Wil Fibrils, while it binds the weakest to CHO cells. In fact, a tenfold greater concentration of heparins was needed to inhibit peptide binding by 50% on Wil fibrils compared to CHO cells (Table 3). In both the CHO and AC10 cell model, less Lovenox was required to yield 50% inhibition of P5+14 binding, compared to full-length heparin.

	Concentration of Heparin or Lovenox at 50% Peptide Inhibition	
Substrate	Heparin	Lovenox
CHO	10 ug/mL	1 ug/mL
Wil Fibrils	33.3 ug/mL	10 ug/mL

Table 3. Inhibition of Peptide P5+14 Binding with Heparin and Lovenox. CHO cells or Wil fibrils were incubated with a serial dilution of heparin or Lovenox with a constant concentration P5+14 for one hour. The values show how much heparin or Lovenox was required to inhibit peptide binding by 50%.

Studies of Synthetic Fibrils on Cardiomyocytes
In order to begin assessing cell surface interactions of amyloid fibrils, AC10 cardiomyocytes were incubated with synthetic Wil fibrils at different concentrations and time points. The physical relationship of the fibrils and cells was visualized by using fluorescently labeled fibrils and phalloidin dye to label the actin cytoskeleton and outline the cell body. Dose- and time-dependent binding was observed (Figures 13 and 14, respectively). At the concentration of 1 μM, the membrane was nearly saturated with fibrils. There was a significant increase in bound fibrils between the 6-hour and 24-hour time points, by which point the cells are covered in fibrils. Moreover, fibrils undoubtedly exhibited strong interactions with the plasma membrane, as is evidenced by the fibrils that bound to the relatively thin membrane extensions and the lack of fibrils bound to the plate. In addition, some brightly fluorescing areas with unclear margins are

located near the nucleus at the highest concentration and time-point (White Arrow, Figure 13). This may be evidence of fibril internalization.
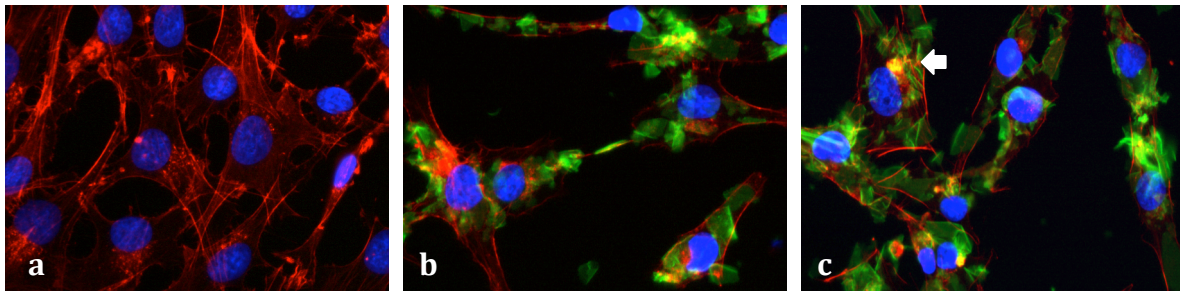

Figure 13. Dose-Dependent Fibril Binding to Cardiomyocytes. AC10 cells were left untreated (A), incubated with green-labeled fibrils at 1 μM (B), or 2 μM (C) overnight, and counterstained with phalloidin (red) and Hoechst 33342 (blue).
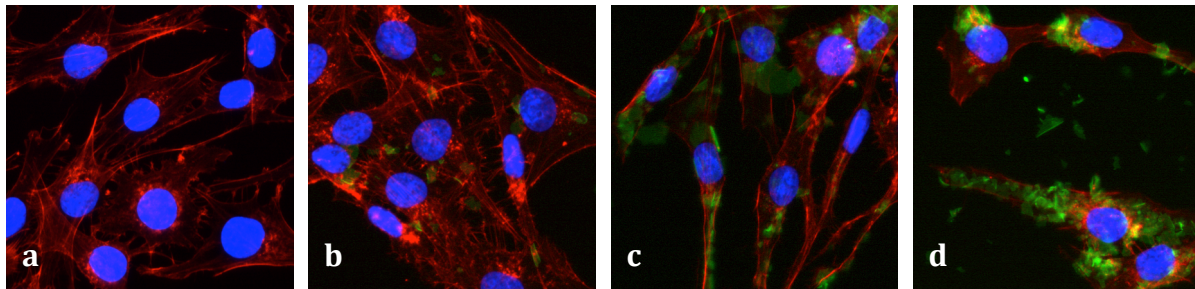

Figure 14. Time-Dependent Binding. AC10 cells were left untreated (A), incubated with labeled fibrils at 1 μM for 1 hour (B), 6 hours (C), or 24 hours (D), and counterstained with phalloidin (red) and Hoechst 33342 (blue).

Pathogenesis of AL Amyloidosis
Light microscopy showed that fibrils bind to AC10 cells in a dose- and time-dependent manner. However, we need to explore whether or not cells internalize amyloid fibrils. If cells do internalize amyloid fibrils, then this could assist in developing hypotheses about amyloid pathogenesis. Furthermore, research should expose how the cell responds to the physical association with amyloid fibrils at the cell surface in order to gain a better understanding of amyloidosis pathogenesis and, more specifically, cytotoxicity.

Localization of the Wil fibrils can be identified using confocal microscopy (Figure 15), which was performed by collaborators at the Oak Ridge National Laboratory. Upon analysis of three coordinates, the fibrils fluoresce brightest at the surface (Z-slice 20); however, some fluorescence is still present at the center of the cell (Z-slice 45). Fibril internalization, therefore, is not the norm. The majority of the fibrils stay at the cell surface, while smaller aggregates may be internalized.
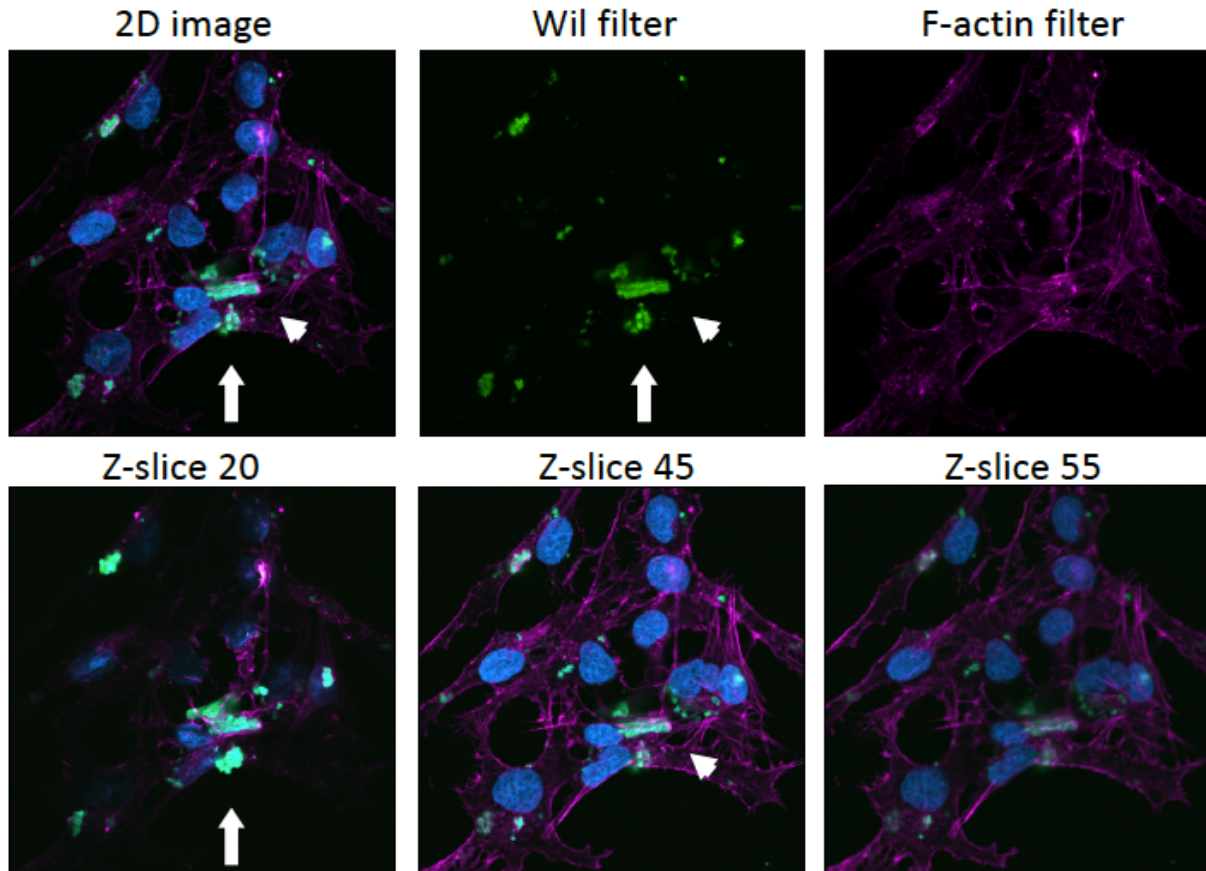
Figure 15. Confocal images for fibril localization. AC10 cells were incubated with 1 μM of Wil fibrils overnight. The cells were then counterstained with phalloidin (red) and Hoechst 33342 (blue). White arrows indicate Wil fibrils associated with the cardiomyocytes.

Oxidative stress has been identified as a side effect of amyloidosis, and McWilliams-Koeppen, et al. showed a significant reduction in NAD(P)H-dependent oxidoreductase activity and decrease in oxygen consumption rate when Wil fibrils bound to AC10 cells. To further investigate, a qualitative measurement of mitochondrial health can be achieved with light microscopy. Mitochondria were stained with MitoTracker Red, which accumulates in active mitochondria and is sequestered as long as a membrane potential is maintained (MitoTracker, 2008). Overall, when cells are incubated with fibrils, they exhibit fewer active mitochondria, which appear to have blurred margins and are more highly concentrated near the nuclei (Figure 16).
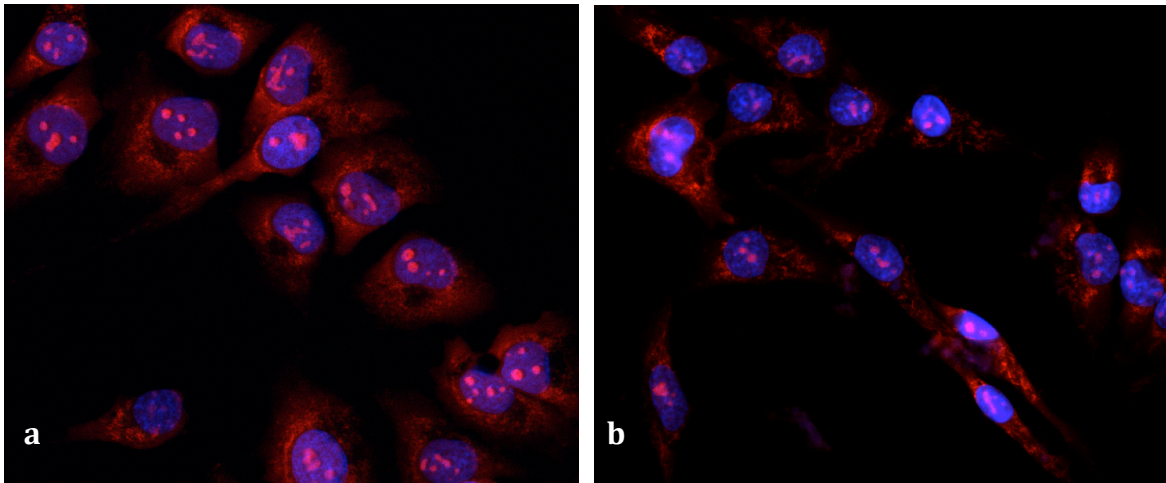
Figure 16. Mitochondrial Health Stain. AC10 cells were left untreated (A), or incubated with Wil fibrils at 1 μM overnight (B), and counterstained with Hoechst 33342 (blue) and MitoTracker Red (red).

As a quantitative measure of mitochondrial health, an MTT assay was run (Figure 17). The MTT assay is considered to be a measurement of cell viability and proliferation, because cells turn purple when mitochondrial dehydrogenases convert MTT into its insoluble purple formazan form, while dead or dying cells cannot carry out this conversion (Mossman, 1983). When compared to a calculation of the area of fibrils bound to each cell at various concentrations, there is a direct inverse relationship between the amount of bound fibrils and mitochondrial health.
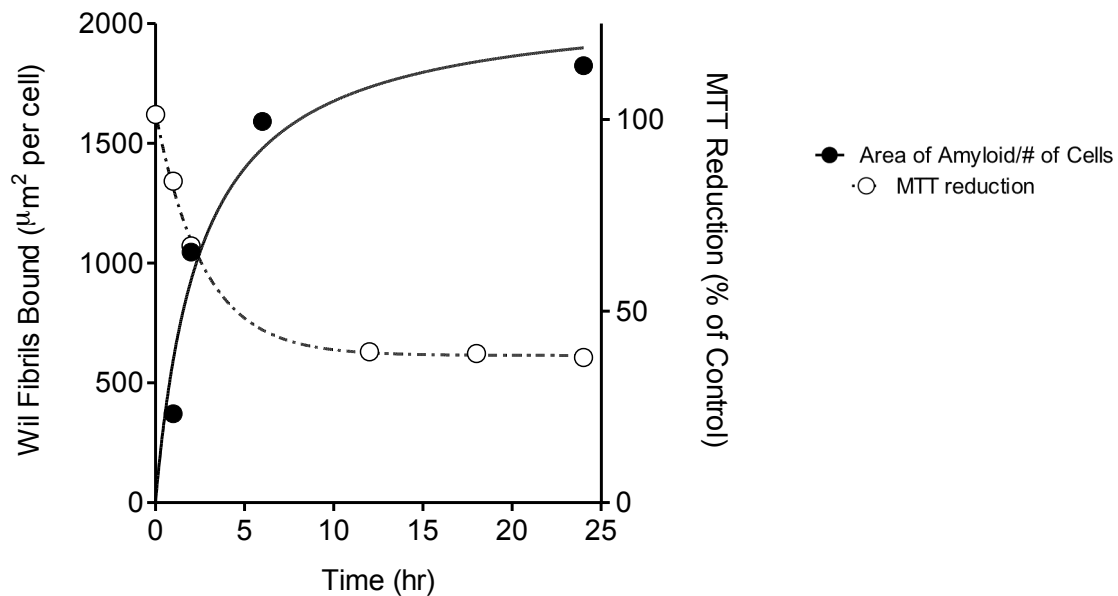
Figure 17. Amyloid Binding over Time to AC10. AC10 cells were incubated with labeled fibrils at 1 μM for 1 hour, 3 hour, 6 hour, and 24 hour. The pictures were analyzed by the ImagePro application, which quantified the number of blue nuclei and calculated the area of green fibrils. Using this acquired data, the area of amyloid per cell was calculated. As a quantitative measure of mitochondrial activity, the MTT assay was performed as given in Materials and Methods and the percent of the maximum optical density was calculated. The fibril-binding and MTT values are presented graphically, and fit with a one phase exponential decay equation.

Apoptosis, or programmed cell death, is one potential consequence of a cell binding to amyloid fibrils. Nuclear blebbing, or disintegration, is one marker of apoptosis, which can be visualized with the Hoechst blue nucleus-specific stain (Figure 18). When cells were left untreated, nuclei morphology appears regular. Generally, the integrity of the nucleus structure is not compromised in response to the addition of fibrils, but there is some cellular debris present, as is evidenced by the small blue dots dispersed throughout (Figure 18B).
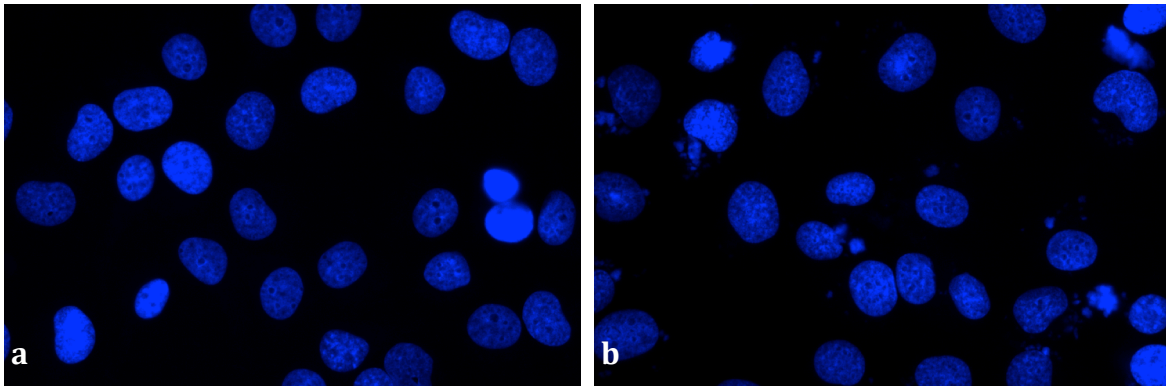

Figure 18. Amyloid fibrils do not generally cause apoptosis. AC10s were left untreated (A), or incubated with 2 μM fibrils for 48 hours (B) and counterstained with Hoechst 33342 (blue). No blebbing nuclei are present; however, cell debris can be observed.

If only a fraction of cells are dying in response to amyloid fibril binding, then can resilient cells still grow and divide while fibrils are attached? Cell counts were compared after 24, 48 and 72 hours of growth on cells that were untreated or incubated with 1 μM of Wil fibrils (Figure 19). Cell division is unimpeded by the addition of the standard concentration of 1 μM Wil fibrils. Interestingly, 5 μM of fibrils causes a significant decrease in cell number after 72 hours of growth (Data not shown).
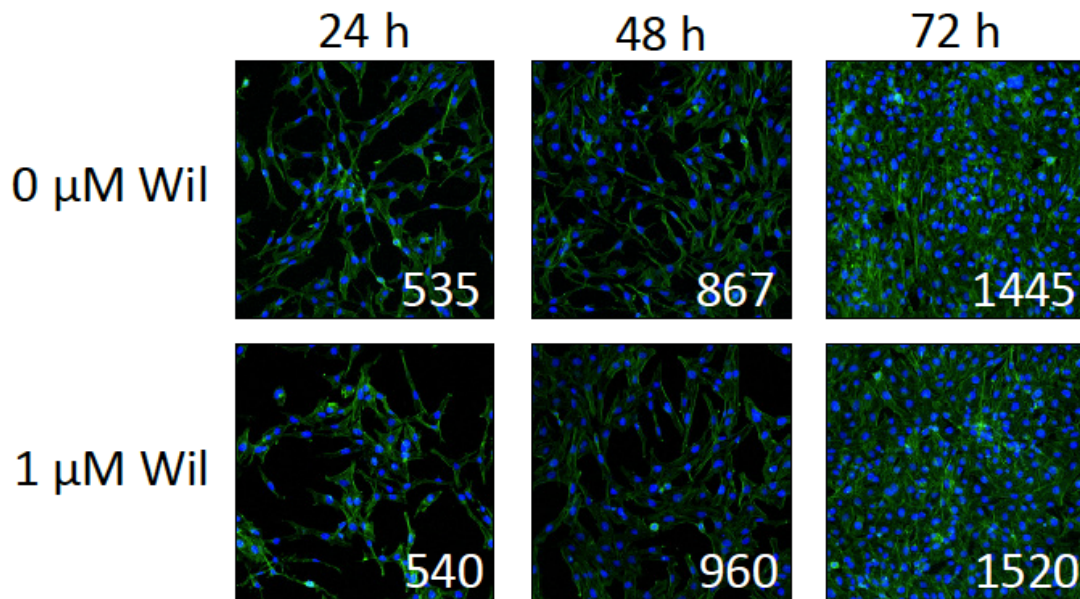

Figure 19. Amyloid fibrils do not affect cell division. AC10 cells were incubated with 0 or 1 μM of non-fluorescent Wil fibril for 24, 48, or 72 hours. Cell counts were performed using the ImagePro application at 100x magnification.

Discussion
Quantitative and qualitative methods revealed that synthetic heparin-binding peptides bind to cells in both a concentration- and time- dependent manner. Meanwhile, a peptide with the same backbone but neutral residues did not exhibit the same binding pattern, suggesting that electrostatic interactions between the peptide and HSPG are the primary force for binding. Future experiments should include a structural analysis of HSPG, so that specific interactions between the synthetic peptides or amyloidogenic proteins and HSPG can be depicted and a more targeted imaging and therapeutic agent can be constructed, if need be.

Enzyme treatments and experiments with cell variants concur in indicating that HSPG are responsible for about 40% of synthetic peptide binding. Enzyme treatment results alone would lead to the conclusion that the HSPG had not fully been digested. However, compounding evidence that the peptide did bind to cells that did not produce HSPG showed that the peptide is interacting with multiple cell surface constituents. In contrast, *in vivo* studies in mouse models have shown that peptide binding is specific to amyloid plaques. *In vitro* studies revealed that factors in serum inhibit peptide binding to cells, but not fibrils, indicating a mechanism by which heparin-binding peptides do not bind to all cells in an individual (Data not shown). The exact mechanisms involved in peptide and fibril binding to the cell and how they confer *in vivo* specificity will be the subject of continuing investigation.

Peptide P5+14 bound to cells, Cab amyloid and Wil fibrils with different affinities. The number of binding sites, or the density of negative charges, available to the peptide can explain this difference. The convoluted extracellular matrix and the highly branched structure of HSPG may be impeding sufficient peptide binding. Cab amyloid extract is "mature" amyloid, meaning the growing aggregate of amyloidogenic monomers associated with other constituents, including heparan sulfate proteoglycans. Conversely, fibrils present tightly packed, similarly oriented and uniform lawn of charges for the alpha helical structure of the peptide to interact with.

Heparin is more highly sulfated than HSPG. However, it has been used as a model of amyloid binding to HSPG, because heparin's modifications are more uniform, better understood, and more apt for ligand binding analyses (Ramirez-Alvarado, 563). This study revealed that heparin and a low molecular weight heparin, Lovenox, were able to competitively inhibit peptide binding to cell surface HSPG. The significant reduction in peptide binding to cells in the presence of heparins confirms that heparin does not serve as a physiologically relevant substitute for HSPG found in healthy individuals or HSPG on cells whose biosynthesis has not yet been altered by amyloidosis. In the future, Isothermal Titration Calorimetry (ITC) could be used to quantitatively measure the energy given off in the form of heat when heparins and synthetic peptides bind.

AL amyloid fibrils also bound to cells in dose- and concentration- dependent manner. The cell surface appeared to be saturated at 1 μM after a 24-hour incubation period. Evidence of internalization emerges only under these "saturated" conditions. Another question to be raised is if internalization leads to apoptosis. Since only a small percentage of cells show evidence of internalization or apoptosis, future studies should determine whether this is a coincidence or due to direct causation. Future studies should also investigate which cellular mechanisms are responsible for the internalization of fibrils. For example, integrin acts as an anchor between the extracellular matrix components and the internal actin cytoskeleton in addition to being the first

step in many signaling cascades (Giancotti, 1999). Thus, integrin is a potential "secondary receptor" for fibrils that may facilitate their internalization. Future experiments could visualize changes in the cytoskeleton in response to amyloid fibrils binding to the cell surface.

Finally, some markers of amyloidosis pathogenesis, including mitochondrial health, apoptosis, and cell division, were tested in this study. A change in the morphology and number of active mitochondria as well as a decrease in MTT fluorescence revealed the oxidative stress felt by cells exposed to amyloid fibrils. Changes in apoptosis and cell division were less severe, and were only observable under more extreme conditions, i.e. at unusually high concentrations of fibrils and after an extended incubation period. The results suggest that cell lysis is not the root cause of AL amyloid pathogenesis, which also suggests that patients with cardiac involvement could expect to recover after amyloid plagues are cleared from their system. Additionally, this data shows that cell surface binding of amyloid fibrils play a role in cytotoxicity. Future experiments should include oligomers and monomers in order to better elucidate amyloid pathogenesis.

All in all, we were able to characterize and visualize the binding of novel synthetic heparin-binding peptides and synthetic amyloid fibrils to cells in this study. In addition, the peptides have a higher affinity to the heparin in solution and fibrils than they do to the cell surface. We also revealed that HSPG is responsible for some, but not all, of the peptide binding. Finally, we showed that fibrils have cytotoxic affects on cells *in vitro*, specifically by causing oxidative stress. However, more questions have been raised than were answered in regards to fibril binding to the cell surface and amyloid pathogenesis. Future studies about the cytotoxicity of amyloid should emphasize physiologically relevant concentrations of amyloid fibrils, because only extreme conditions yielded significant changes in cellular function in this study. In addition, comparative studies involving different types of amyloidogenic proteins may reveal a better general mechanism of amyloid fibrillization and deposition.

References
Ancsin, J. (2003). Amyloidogenesis: historical and modern observations point to heparin sulfate proteoglycans as a major culprit. *Amyloid: Journal of Protein Folding Disorders* 10(**2**):67-79.

Ancsin, J., Kisilevsky, R. (1999). The Heparin/Heparan Sulfate-binding Site on Apo-serum Amyloid A: Implications for the Therapeutic Intervention of Amyloidosis. *Journal of Biological Chemistry* **274**:7172-7181.

Castillo, G.M., Cummings, J.A., Yang, W., Judge, M.E., Sheardown, M.J., Rimvall, K., Hansen, J.B., Snow, A.D. (1998). Sulfate content and specific glycosaminoglycan backbone of perlecan are critical for perlecan's enhancement of islet amyloid polypeptide (amylin) fibril formation. *Diabetes* 47(**4**):612-620.

Chargaff, E. (1938). Studies on the Chemistry of Blood Coagulation: Protamines and Blood Clotting. *The Journal of Biological Chemistry* **125**:671-676.

Dahlen, P. (1987). Detection of Biotinylated DNA Probes by Using Eu-Labeled Streptavidin and Time-Resolved Fluorometry. *Analytical Biochemistry* **164**: 78-83.

Dubrey, S.W., Cha, K., Anderson, J., Chamarthi, B., Reisinger, J., Skinner, M., Falk, R.H. (1998). The clinical features of immunoglobulin light chain (AL) amyloidosis with heart involvement. *Q J Med* **91**:141-157.

Fraser, P.E., Nguyen, J.T., Chin, D.T., Kirschner, D.A. (1992). Effects of sulfate ions on Alzheimer β/A4 peptide assemblies: Implications for amyloid fibril-proteoglycan interactions. *Journal of Neurochemistry* **59**:1531-1540.

Gandhi, N., Mancera, R. (2008). The Structure of Glycosaminoglycans and their Interactions with Proteins. *Chem Biol Drug Design* **72**:455-482.

Giancotti, F., Ruoslahti, E. (1999). Integrin Signaling. *Science* 285(**5430**):1028-1033.

Gupta-Bansal, R., Frederickson, R.C., Brunden, K.R. (1995). Proteoglycan-mediated inhibition of Aβ proteolysis. A potential cause of senile plaque accumulation. *Journal of Biological Chemistry* **270**:18666-18671.

Kisilevsky, R., Ancsin, J., Szarek, W., Petanceska, S. (2007). Heparan sulfate as a therapeutic target in amyloidogenesis: prospects and possible complications. *Amyloid* 14(**1**)21-32.

Lacy, M., Dispenzieri, A., Hayman, S., Kumar, S., Kyle, R., Rajkumar, S., Edwards, B., Rodeheffer, R., Frantz, R., Kushwaha, S., Clavell, A., Dearant, J., Sundt, T., Daly, R., McGregor, C., Gastineau, D., Litzow, M., Gertz, M. (2008). Autologous Stem Cell Transplant

after Heart Transplantation for Light Chain (AL) Amyloid Cardiomyopathy. *The Journal of Heart and Lung Transplantation* 27(8):823-829.

Lindahl, B., Lindahl, U. (1997). Amyloid-specific Heparan Sulfate from Human Liver and Spleen. *Journal of Biological Chemistry* **272**:26091-26094.

McWilliams-Koeppen, H., Foster, J.S., Hackenbrack, N., Ramirez-Alvarado, M., Donhoe, D., Williams, A., Macy, S., Wooliver, C., Wortham, D., Morrell-Falvey, J., Foster, C., Kennel, S., Wall, J. Immunoglobulin light chain fibrils cause metabolic dysfunction in human cardiomyocytes without cell death. *PLOS ONE*. Accepted.

Merlini, G., Bellotti, V. (2003). Mechanisms of Disease: Molecular Mechanisms of Amyloidosis. *The New England Journal of Medicine* **349**:583-596.

MitoTracker Mitochondrion-Selective Probes (2008). Molecular Probes: Invitrogen Detective Technologies. <http://tools.lifetechnologies.com/content/sfs/manuals/mp07510.pdf>.

Mossman, T. (1983). Rapid calorimetric assay for cellular growth and survival: application to proliferation and cytotoxic assays. *Journal of Immunological Methods* **65**:55-63.

Mumford, A., et al. (2000). Bleeding symptoms and coagulation abnormalities in 337 patients with AL-amyloidosis. *British Journal of Haematology* 11(**2**):454-460.

Pokkulurim P.R., Soloman, A., Weiss, D.T., Stevens, F.J., Schiffer, M. (1999). Tertiary structure of human λ6 light chains. *Amyloid* **6**: 165-171.

Ramirez-Alvarado, M., Kelly, J., Dobson, C. (2010). Protein Misfolding Diseases: Current and Emerging Principles and Therapies. 1st Edition. Wiley.

Sanchorawala, V. (2006). Light-Chain (AL) Amyloidosis: Diagnosis and Treatment. *Clinical Journal of the American Society of Nephrology* 1(**6**):1331-1341.

Silva, L., Khomandiak, S., Ashbrook, A., Weller, R., Heise, M., Morrison, T., Dermody, T. (2013). A Single-Amino-Acid Polymorphism in Chikungunya Virus E2 Glycoprotein Influences Glycosaminoglycan Utilization. *Journal of Virology* 88(**5**):2385.

Wall, J., Martin, E., Richey, T., Stuckey, A., Macy, S., Wooliver, C., Williams, A., Foster, J., McWilliams-Koeppen, P., Uberbacher, E., Cheng, X., Kennel, S. (2015). Preclinical validation of the heparin-reactive peptide p5+14 as a molecular imaging agent for visceral amyloidosis. *Molecules* **20**. Accepted.

Wall, J., Richey, T., Stuckey, A., Donnell, R., Macy, S., Martin, E., Williams, A., Higuchi, K., Kennel, S. (2011). In vivo molecular imaging of peripheral amyloidosis using heparin-binding peptides. *PNAS* 108(**34**):E586-594.

Wall, J., Richey, T., Stuckey, A., Donnell, R., Oosterhof, A., van Kuppevelt, T., Smits, N., Kennel, S. (2012). SPECT imaging of peripheral amyloid in mice by targeting hyper-sulfated heparin sulfate proteoglycans with specific scFv antibodies. *Nucl Med Biol* 39(**1**):65-75.

Wall, J., Schell, M., Murphy, C., Hrncic, R., Stevens, F., Solomon, A. (1999). Thermodynamic Instability of Human λ6 Light Chains: Correlation with Fibrillogenicity. *Biochemistry* **38**: 14101-14108.

Yamaguchi, I. Suda, H., Tsuzuike, N., Seto, K., Seki, M., Yamaguchi, Y., Hasegawa, K., Takahasi, N., Yamamoto, S., Gejyo, F., Naiki, H. (2003). Glycosaminoglycan and proteoglycan inhibit the depolymerization of beta2-microglobulin amyloid fibrils in vitro. *Kidney International* **64**:1080-1088.